



**HAL**  
open science

## GLAND AND ZONAL SEGMENTATION OF PROSTATE ON T2W MR IMAGES

O. Chilali, Pascal Puech, S Lakroum, M. Diaf, S. Mordon, N. Betrouni

► **To cite this version:**

O. Chilali, Pascal Puech, S Lakroum, M. Diaf, S. Mordon, et al.. GLAND AND ZONAL SEGMENTATION OF PROSTATE ON T2W MR IMAGES . J Digit Imaging, 2016. hal-01341867

**HAL Id: hal-01341867**

**<https://hal.science/hal-01341867>**

Submitted on 5 Jul 2016

**HAL** is a multi-disciplinary open access archive for the deposit and dissemination of scientific research documents, whether they are published or not. The documents may come from teaching and research institutions in France or abroad, or from public or private research centers.

L'archive ouverte pluridisciplinaire **HAL**, est destinée au dépôt et à la diffusion de documents scientifiques de niveau recherche, publiés ou non, émanant des établissements d'enseignement et de recherche français ou étrangers, des laboratoires publics ou privés.

# GLAND AND ZONAL SEGMENTATION OF PROSTATE ON T2W MR IMAGES

*Chilali O.<sup>1,4</sup>, Puech P<sup>1,2,3</sup>, Lakroum S.<sup>1</sup>, Diaf M.<sup>4</sup>, Mordon S.<sup>1,2</sup>, Betrouni N.<sup>1,2</sup>*

<sup>1</sup>Inserm, U1189, F59000, Lille, France.

<sup>2</sup>Univ. Lille, U1189 – ONCO-THAI – Image Assisted Laser Therapy for Oncology, F-59000 Lille, France.

<sup>3</sup>CHU Lille, Radiology Department, Claude Huriez Hospital, F-59000 Lille, France.

<sup>4</sup>Automatic Department, Mouloud Mammeri University, Tizi-Ouzou, Algeria

## **Corresponding Author**

Nacim Betrouni, PhD

INSERM U1189

1, avenue Oscar Lambret

59037, Lille, France.

Telephone number: +33 320 446 722

Fax number: 33 320 446 738

E-mail: [nacim.betrouni@inserm.fr](mailto:nacim.betrouni@inserm.fr)

**Abstract**—For many years, prostate segmentation on MR images concerned only the extraction of the entire gland. Currently, in the focal treatment era, there is a continuously increasing need for the separation of the different parts of the organ. In this paper, we propose an automatic segmentation method based on the use of T2W images and atlas images to segment the prostate and to isolate the peripheral and transition zones. The algorithm consists of two stages. First, the target image is registered with each zonal atlas image then the segmentation is obtained by the application of an evidential C-Means clustering. The method was evaluated on a representative and multi-centric images base and yielded mean Dice accuracy values of 0.81, 0.70 and 0.62 for the prostate, the transition zone and peripheral zone respectively.

**Key words:** Prostate, MR T2W images, segmentation, zones, Atlas.

## I. INTRODUCTION

One of the latest trends in prostate cancer management is the concept of focal therapy aiming to target only the subpart of the gland with the cancerous lesions. The development of such techniques needs a precise estimation of the cancer localizations maps. Multimodality imaging and mainly multiparametric magnetic resonance images (mpMRI) are efficient tools to this end. Computer aided diagnosis (CAD) software solutions were widely investigated to help in images analysis. Many works focused on prostate extraction from the images and different techniques are now able to automatically segment the prostate with a sufficient accuracy [1].

On the other side, prostate is a heterogeneous organ formed by three main areas: the central area, the transition zone and the peripheral zone [2]. The transition zone and the central zone are usually referred as the central gland. Here, we consider them as the transition zone (TZ). The peripheral zone (PZ) is the area where most prostate cancers grow [3]. Moreover, cancers of these two zones exhibit different behaviors [4]. Thus, it appears important to separate them in order to apply different analysis algorithms. However, oppositely to the gland segmentation problem, fewer studies focused on this issue. Indeed, the first study was proposed in 2011 [5]. The authors combined the mpMR images and incorporated them into a segmentation process based on the evidential C-Means classifier. Later on, other works ([6], [7]) introduced different techniques also based on mpMRI.

In ([8], [9] and [10]), the authors proposed new approaches based only on the T2-weighted (T2W) MR sequence, because these images are regarded as the cornerstone for prostate morphology evaluation. However, due to the lack of contrast between the two zones, the accurate segmentation of the two zones using only T2W images remains challenging. Additional information as *a priori* information can guide the segmentation process. In this study, starting from the initial work [5], we use the Evidential C-Means classifier to segment the PZ and TZ using only the T2 weighted sequence. *A priori* information about the prostate morphology is modelled using an atlas [11], the ProstateAtlas (publicly available at the prostateWeb URL [12]).

## II. METHODS

The global approach is based on two major components; the first is a registration step aiming to align the target image i.e., the image to be segmented with the atlas image while the second is a classification step aiming to drive the segmentation. Figure 1 shows the outline of the proposed method.

### II-1 Registration

The registration step aims to obtain an automatic initialization. It is done using the ProstateAtlas. This atlas, described in [11], was constructed starting from 30 T2 weighted MR images. The images were selected as representative of the prostate cancer patients' population. Patients were selected in term of age, prostate volume and prostate appearance. The result is a mean T2 weighted grey level image and a probabilistic distribution (atlas) image for each zone. These probabilistic distributions model the inter-patient variability.

The atlas mean image is registered using an affine transformation with the target T2W image and the obtained optimal transformation is applied to the two zone atlases in order to spatially match them with the target image. This matching allows the labelling of the corresponding voxels of the target image with their corresponding probabilities to belong to each zone (class). The labelling is considered as a first solution and acts as initialization for the clustering process.

### II-2 Clustering and Segmentation

Starting from the initialization obtained after the registration, this step consists in a classification process to optimize the target image voxels labelling. In order to reduce the search space, a first treatment is applied to extract the prostate from the image. As it was highlighted in the introduction, prostate segmentation from MR images was very widely discussed and different efficient algorithms were published. We applied here one of these methods which was among the first to be proposed [13]. It combines a priori knowledge of prostate shape and Markov fields modelling to guide an Iterative Conditional Mode algorithm and to perform a Bayesian classification.

For the zonal segmentation, we chose to adapt the first applied technique based on evidence theory [5]. Evidential reasoning, also known as belief functions theory or Dempster-Shafer theory, provides an advanced modelling of fusion, conflicts between sources, and outliers.

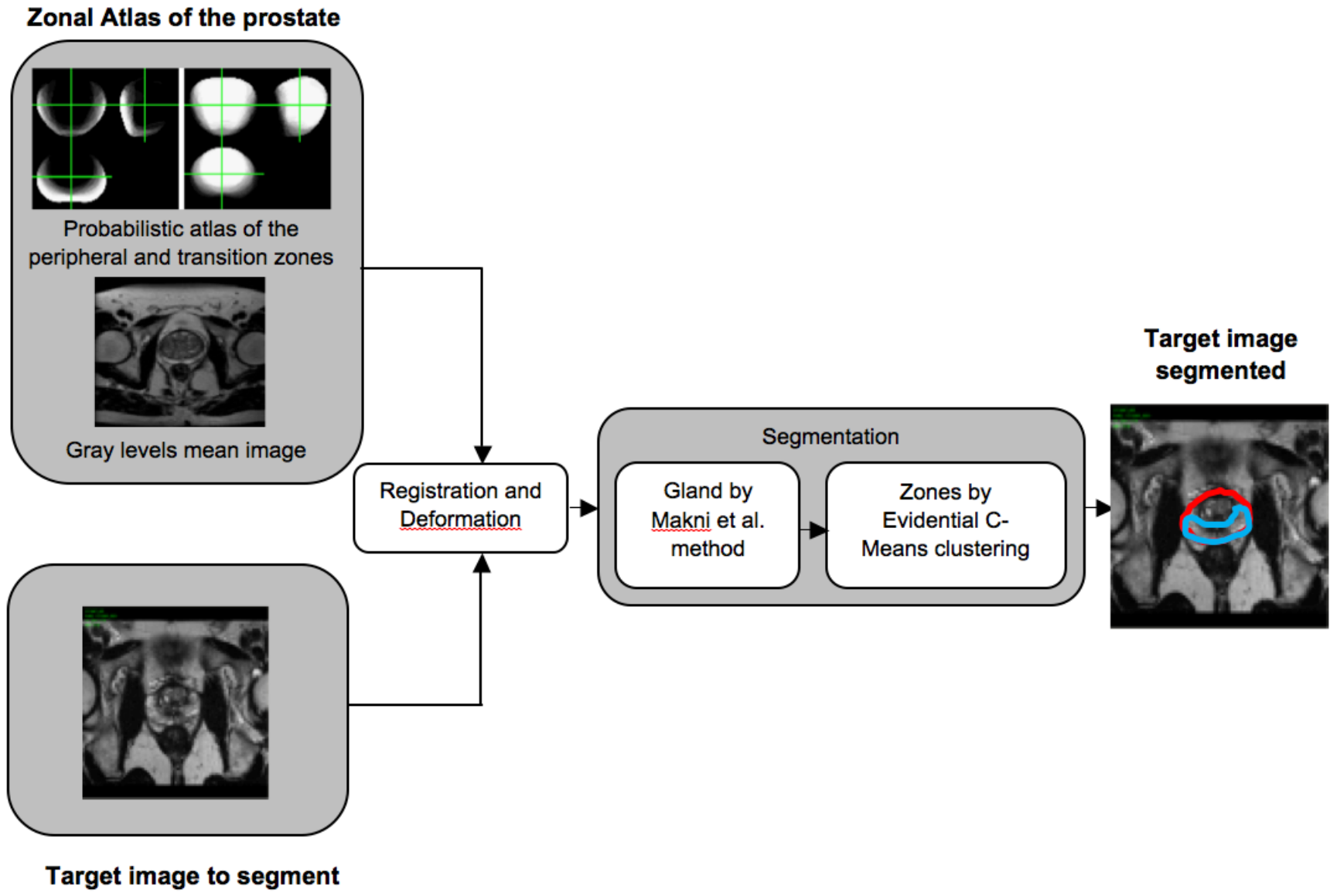


**Figure 1.** Block diagram of the proposed prostate zonal segmentation method.

## II-2-a Evidential Modelling

This modelling associates a data source or sensor  $S$  with a set of propositions, also known as the “frame of discernment”. In a classification context, the frame of discernment  $\Omega$  is the classes set  $\omega_i$ ,  $\Omega = \{\omega_1, \dots, \omega_k\}$ .

If we define  $P = \{P_1, \dots, P_N\}$  as the set of patterns/objects to be assigned to one of the classes of  $\Omega$ , then evidential reasoning allows to extract a partial knowledge on this assignment, called “basic belief assignment” (*bba*). A *bba*, is a function that takes values in the range  $[0, 1]$ . For each pattern  $P_i \in P$ , a *bba*, that we note  $m_i$ , allows to measure its assignment to each subset  $A$  of  $\Omega$  such as:

$$\sum_{A \subseteq \Omega} m_i(A) = 1 \quad (1)$$

The higher the value of  $m_i(A)$ , the stronger the belief on assigning  $P_i$  to  $A$ . Compared to the fuzzy sets model, the evidential reasoning is then capable of extending the concept of partial membership by assigning belief not only to classes but also to unions (disjunctions) of classes.

Using this model, Denoeux and Masson [14] introduced a new kind of data partition called the “Credal partition”. This partition could be seen as an extension of the fuzzy partitions with *bbas* replacing fuzzy membership functions. Later on, the authors proposed an evidential version of the C-Means classifier that uses a credal partition. This evidential classifier, inspired by the fuzzy C-Means (FCM), is called ECM [15]. Its principle is to classify the  $N$  patterns into  $k$  classes of  $\Omega$  based on classes’ centers and the minimization of a cost function. As for fuzzy partitions in FCM, a credal partition, in which each line is a *bba*  $m_i$  associated to a pattern  $P_i$ , is optimized in an iterative process.

## II-2-b From classification to segmentation

In the current application, each pattern is a voxel from the MR T2 weighted image. The classification process classifies the patterns into 2 classes:  $\omega_1$  for the peripheral zone, and  $\omega_2$  for the transition zone. For each pattern, a *bba* measures the amount of belief assigned to:

- class  $\omega_1$  : the pattern is a voxel from the PZ;

- class  $\omega_2$  : the pattern is a voxel from the TZ;
- the set  $\{\omega_1, \omega_2\}$ : all hypotheses hold: the pattern may be a voxel from PZ or TZ.
- the empty set  $\phi$ : pattern is considered as outlier and rejected.

The ECM model extracts and optimizes partial knowledge on patterns' assignment. A direct use of the ECM would classify voxels as independent data objects. However, voxels neighborhood, as defined by a connexity system, brings valuable information. We assume that in a homogeneous region or class, a *bba* is not only a knowledge on a pattern, but also on its connected neighbors. Corrupted information, extracted from outliers/noise patterns, can be relaxed by information from its neighbors, which is one of the principles of noise-reducing methods and filters. Thus, introducing neighborhood information in the ECM modelling would assimilate the ECM classifier to a region-based segmentation process.

The *bbam<sub>i</sub>* of pattern  $P_i$ (associated to voxel  $v_i$ ) is relaxed by combining it with *bbas* from spatially connected neighbors. Spatial connection is defined by a 26-connexity system. However, the contribution of each neighbor of to this combination should be weighted by the distance that spatially separates the corresponding voxels. This is particularly relevant in case of prostate MRI, where voxels are significantly anisotropic. The further the voxel, the less it should contribute to the combination.

This combination will be used as a relaxation step that allows correcting the evidential assignment of a voxel based on information from its neighbors. We propose to introduce this relaxation into the iterative process of the ECM in the following way:

$$m_i = \frac{1}{26} \left( m_i + \sum_{j=1}^{26} m_j \cdot d_j \right) \quad (2)$$

Where  $d_j$  is the Euclidean distance between voxel  $v_i$  and its spatial neighbor  $v_j$

At the level of *bbas* extraction and optimization, we measure belief on the membership of each voxel to one of the classes  $\omega \in \Omega$  but we also measure belief on rejection ( $\emptyset$ ), and disjunctions  $A \subseteq \Omega$  which can be interpreted as 'doubt' on the membership of the voxel. A decision still has to be made to classify the voxels to one of the classes of  $\Omega$ . The decision level can be reached by transforming the *bbas*  $m_i$  into a probability measure. This probability is calculated as:

$$Prob(w_i) = \frac{1}{1 - m_i(\phi)} \sum_{\substack{\omega \in A \\ A \subseteq \Omega}} \frac{m_i(A)}{|A|}, \quad \forall \omega_i \in \Omega \quad (3)$$

where  $|A|$  denotes the number of elements of  $A$ . We finally define the decision rule  $R$  by:

$$R(P_i, m_i) = \underset{\omega \in \Omega}{argmax} (Prob(\omega_i)) \quad (4)$$

### III. EXPERIMENTS AND RESULTS

For the validation of the method, two databases were considered. The first, containing images from 13 patients, was from MICCAI 2012 Challenge (PROMISE 2012)[16] (Table 1). The second was a multi-centric database, collected from 5 sites. It was composed of images from 22 patients (Table 2). As prostate appearance on the images is impacted by different parameters as the patient age and the final cancer diagnosis, images were selected in a way to be representative of the population. Thus, patients were in the age range (45-68) years with a mean age of 56, while prostate volumes were in the range (24-82)  $\text{cm}^3$  with mean volume of 43  $\text{cm}^3$ . For diagnosis outcome, 14 patients (63.6%) had been diagnosed “positive” for cancer.

Images were acquired with standard T2W sequences as proposed by the different manufacturers.

TABLE 1. PARAMETERS OF THE MICCAI CHALLENGE MR DATABASE.

Patients	Voxel size ( $\text{mm}^3$ )	Image size (voxel)
1-4, 6, 7	0.625x0.625x3.6	320x320x20
5	0.625x0.625x3.6	320x320x20
8-10	0.39x0.39x3.3	512x512x23
11	0.468x0.468x3.33	384x384x28
12	0.351x0.351x3.3	512x512x26
13	0.625x0.625x3.6	320x320x28

TABLE 2. PARAMETERS OF THE MULTI-CENTRIC MR DATABASE.

Patients	Device	Voxel size (mm <sup>3</sup> )	Image size (voxel)
1-4, 6-15	Philips 1.5T	0.31x0.31x4	512x512x15
5, 17-20	Siemens 1.5T	0.78x0.78x3	256x256x24
16	GE 1.5T	0.39x0.39x3	512x512x22
21	GE 3T	0.47x0.47x4	512x512x15
22	GE 3T	0.74x0.74x4	512x512x20

Evaluation is done by comparing the segmentation result noted  $V_s$  to a reference  $V_r$ , using the following criteria:

- Overlap Ratio (OR) also known as Jaccard index, is the ratio of the intersection's volume to the union's volume (optimal value = 1):

$$OR = \frac{|V_r \cap V_s|}{|V_r \cup V_s|} \quad (5)$$

- Dice Similarity Coefficient (DSC) is a similarity measure based on the Jaccard index (optimal value=1), defined by:

$$DSC = \frac{2 \cdot |V_r \cap V_s|}{|V_r| + |V_s|} \quad (6)$$

- Mean Euclidean distance (DIST) between the contours (automatic and manual) drawn on the same MR image. The center of gravity of the manual contour was chosen as a reference point. Straight-line segments intersected the two contours. The intersection points were considered to compute DIST.

The PROMISE database served to highlight the performance of the gland extraction step in the proposed method (Table 3). The reference segmentation was available for these data.

For the second database, the obtained results were compared with manual segmentations produced by an expert radiologist (more than 15 years' experience) (Table 4).

TABLE 3. OVERALL PERFORMANCE RESULTS ON THE MICCAI DATABASE.

Patient	DSC (%)	DIST (mm)
Patient 1	74.13	4.3
Patient 2	74.59	4.5
Patient 3	66.82	4.8
Patient 4	76.95	4.3
Patient 5	71.30	4.5
Patient 6	85.57	2.8
Patient 7	72.96	3.9
Patient 8	82.26	3.0
Patient 9	83.69	3.1
Patient 10	75.07	4.2
Patient 11	79.43	3.85
Patient 12	78.93	3.8
Patient 13	79.63	3.15
Mean	<b>77.02 ± 5.26</b>	<b>3.8</b>

TABLE 4. OVERALL PERFORMANCE RESULTS FOR THE 22 PATIENTS OF DATABASE 2.

	DSC (%)	OR (%)	DIST (mm)
Prostate	81.78±5.86	69.57±8.14	3.00±1.5
TZ	70.23±12.06	64.40±13.44	4.5±1.8
PZ	62.00±7.27	57.30±11.60	5.2±2.7

For both patients bases, the execution time was  $15 \pm 5$ s (mean  $\pm$  SD) for the registration step and about  $50 \pm 5$ s (mean  $\pm$  SD) for the segmentation step, giving an overall execution time of less than 2 minutes for the whole process.

Figure 2 depicts the results for two patients from the two databases. Figure 3 shows a mutual display of the segmentation result of the patient from the PROMISE 12 database, overlaid on the central image.

#### IV. DISCUSSION

In this study, we investigated the abilities of the combination of evidential clustering and prostate zonal atlases to drive a segmentation process for separating the peripheral and the transition zones on T2 weighted MR Images. Compared to the previous published studies, the current one brings two novelties. First, it operates only on the T2 weighted sequence while the most previous methods require multiparametric data. The second consists in the introduction of probabilistic atlases of the two zones. This approach was inspired by the techniques used for gray and white matters segmentation on brain MR imaging.

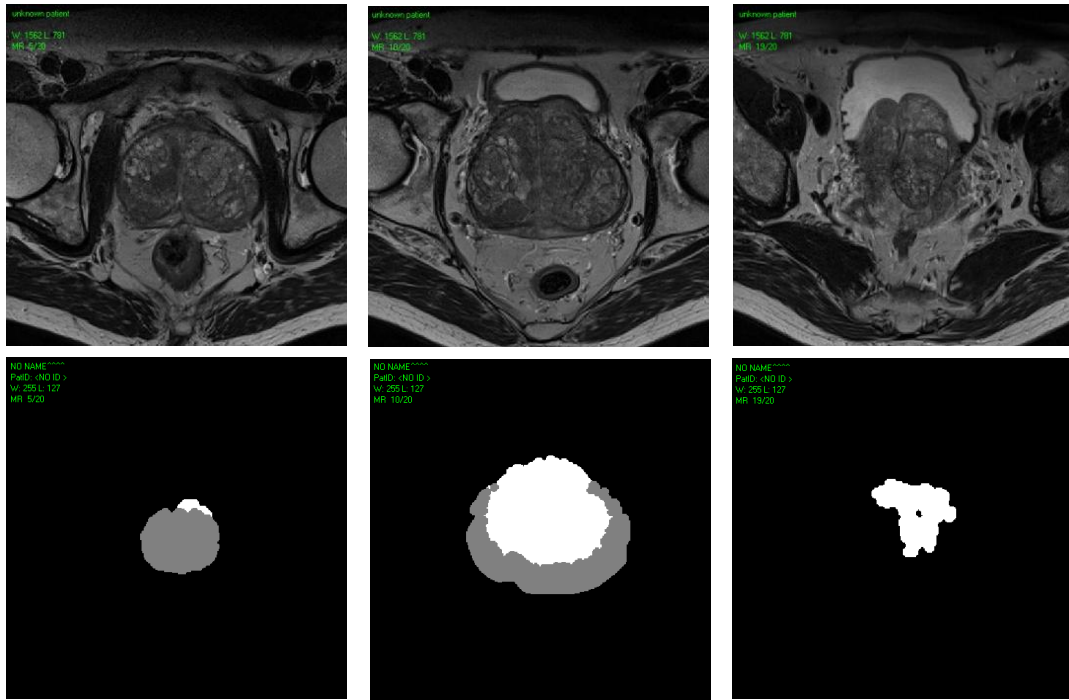
The First step of the method involves a gland extraction where we have applied the method described in [13]. When applied on the PROMISE 12 challenge data, the method exhibits performances (Table 3, mean DSC=77%) within the range of the reported values (65 % -84 %) [1].

For the zonal segmentation, the overall results of the proposed method (Table 4) could appear insufficient mainly for the peripheral zone extraction (mean DSC 62%). However it must be stressed that these results were obtained on an image base that reflects the real life images: different appearances and volumes of the prostates. The algorithm results are very close to the expert contours in the central part of the gland. Nevertheless, for the prostate extremities: the base and mainly the apex, the results are poor. This is mainly due to the lack of signal and the partial volume effect. The enhancement of image qualities by the development of new image sequences and new images reconstruction algorithm will certainly improve the signal to noise ration ratio leading to an improvement of the segmentation.

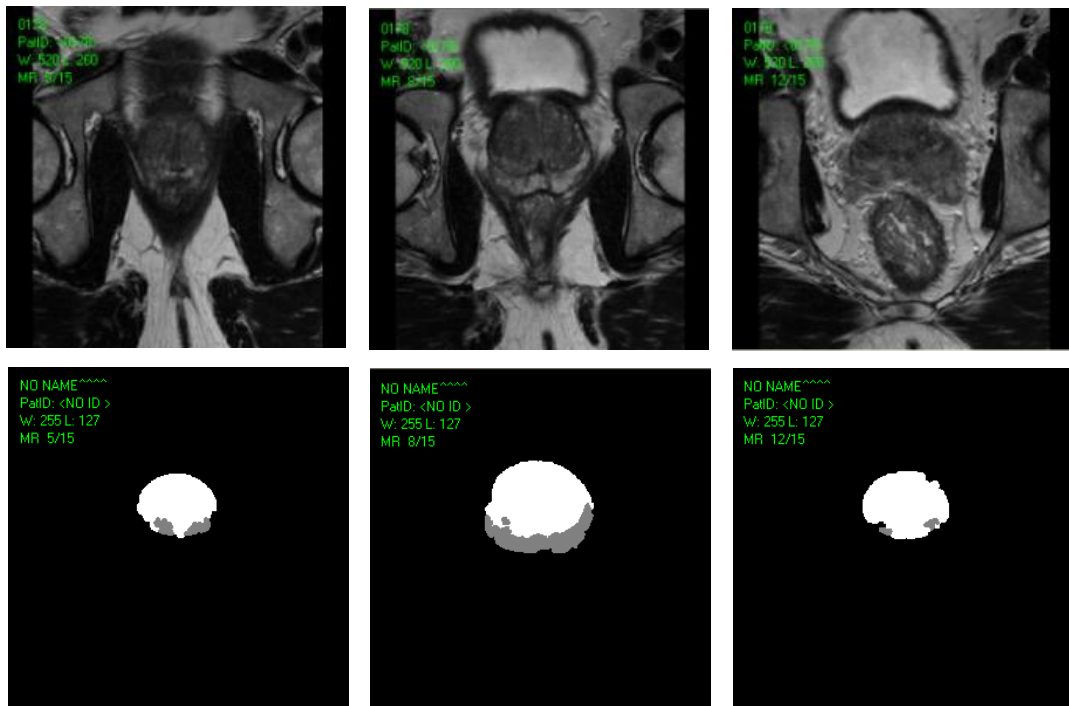
Another issue that can be seen as a limit of this study is the validation using only a single expert while currently the trend is to take into account the inter-observer variability through STAPLE techniques for instance. Most often, the use of multi-observer references is done by generating a pseudo ground-truth reference taking into account all the references. This consensus reference can be seen as a mean contour that normalizes the most experienced observers' contours with those produced by the observers with limited experience. We chose to perform the validation by comparison to manual delineations done by an experienced radiologist (second author). He used multiparametric and multi-incidence MR images, with

transverse, sagittal and coronal slices, to draw the contours as accurately as possible. Moreover, it is important to stress that in daily clinical practice, diagnosis and therapies planning tasks are based on a single user.

Lastly to conclude, the main aim of this work was to propose a simple technique, suitable to clinical conditions (mean execution time less than 2 minutes) to perform complete segmentation of the gland and the extraction of the peripheral and transition zones. The all process is fully automatic even if in some cases, after convergence some manual corrections are needed at the gland extremities.



(a)



(b)

**Figure 2.** Results of the two zones segmentation: the transition region (white region), the peripheral region (gray region). From left to right: the apex, the central slice and the base. (a) Patient 6 from the MICCAI challenge database (Prostate's DSC =85.57%, PZ's DSC=51.20% and TZ's DSC=74.40%), (b) Patient 13 from the multi-centric MR database (Prostate's DSC=88.80%, PZ's DSC=71.30% and TZ's DSC=84.20%).

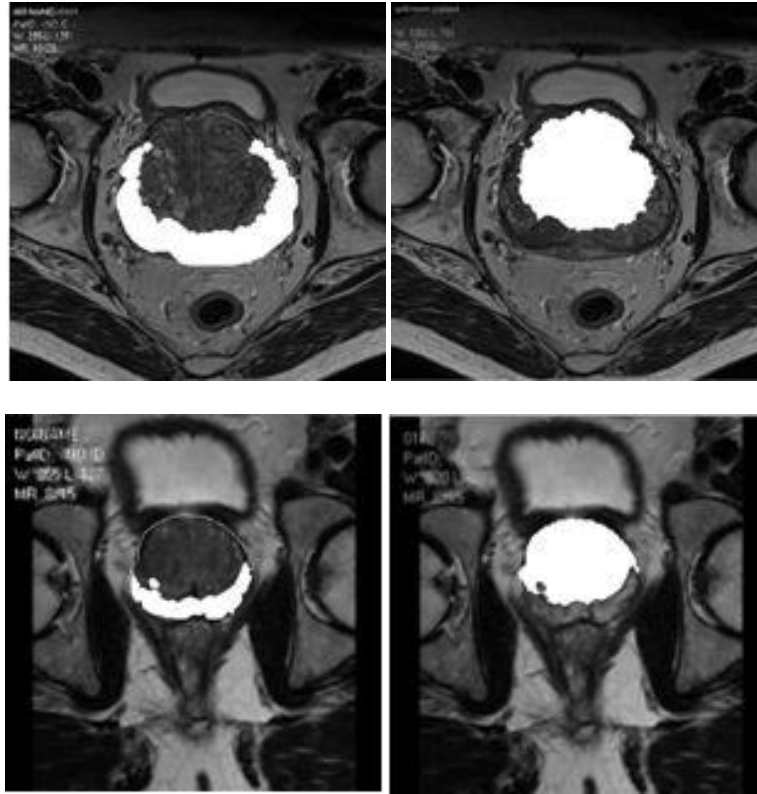


**Figure 3.** Combined display of the segmentation results overlaid on the T2 weighted image for the central slice. The first column shows the peripheral zone and the second the transition zone. Patient 6 from the MICCAI challenge database (Prostate's DSC =85.57%, PZ's DSC=51.20% and TZ's DSC=74.40%).

## References

- [1] Litjens G., Toth R. B., van de Ven W. A., Hoeks C. A., Kerkstra S. A. B, van Ginneken R. A, Vincent G. Evaluation of prostate segmentation algorithms for MRI: The PROMISE12 challenge. *Medical Image Analysis* 18:359-373, 2014.
- [2] Yacoub J. H., Verma S., Moulton J. S., Eggener S., Aytekin O. Imaging-guided prostate biopsy: conventional and emerging techniques. *RadioGraphics* 32:819–837, 2012.
- [3] Haffner J, Potiron E., Bouyé S., Puech P., Leroy X., Lemaitre L., Villers A. Peripheral zone prostate cancers: location and intraprostatic patterns of spread at histology. *Prostate* 69 (3):276-282, 2009.
- [4] Sakai I., Ken-ichi H., Hara I., Eto H., Miyake H. A comparison of the biological features between prostate cancers arising in the transition and peripheral zones. *British Journal of Urology* 96:528-532, 2005.
- [5] Makni N., Iancu A., Colot O., Puech P., Mordon S. and Betrouni N. Zonal segmentation of prostate using multispectral magnetic resonance images. *Medical Physics* 38(11): 6093-6105, 2011.
- [6] Litjens G., Debats O., Van de Ven W., Karssemeijer N. and Huisman H. A pattern recognition approach to zonal segmentation of the prostate on MRI, *Medical Image Computing and Computer-Assisted intervention (MICCAI)*, Part II. LNCS 7511, 413-420, 2012.
- [7] Maan B., Van der Heijden F. and Futterer J. J. A new prostate segmentation approach using multispectral magnetic resonance imaging and a statistical pattern classifier. *Proc.of SPIE* 8314 1-9, 2012.
- [8] Toth R., Ribault J., Gentile J., Sperling D. and Madabhushi A. Simultaneous segmentation of prostatic zones using Active Appearance models with multiple coupled level sets. *Computer Vision and Image understanding* 117:1051-1060, 2013.
- [9] Qiu W., Yuan J., Ukwatta E., Sun Y., Rajchl M. and Fenster A. Efficient 3D multi-region prostate MRI segmentation using dual optimization. *IPMI 2013(LNCS 7917)*:304-315, 2013.
- [10] Yuan J., Ukwatta E., Qui W., Rajchl M. and Sun Y. Jointly segmenting prostate zones in 3D MRIs by globally optimized coupled level-sets. *EMMCVPR LNCS 8081*:12-25, 2013.
- [11] Betrouni N., Iancu A., Puech P., Mordon S., Makni N. ProstAtlas: A digital morphologic atlas of the prostate. *Eur.J.Radiol.* 81(9):1969-1975, 2012.
- [12] <http://www.metadataweb.onco-thai.fr>
- [13] Makni N., Puech P., Lopes R., Viard R., Colot O. and Betrouni N. Combining a deformable model and a probabilistic framework for an automatic 3 d segmentation of prostate on MRI. *International Journal of Computer Assisted Radiology and Surgery* 4 :181-188, 2009.
- [14] Denoeux T. and Masson M. -H. Evidential clustering of proximity data. *IEEE Transactions on Systems, Man and Cybernetics* 34:95-109, 2004.
- [15] Masson M.-H. and Denoeux T. ECM : An evidential version of the fuzzy c-means algorithm. *Pattern Recognition* 41:1384-1397, 2011.
- [16] <http://promise12.grand-challenge.org/Download/showSection/data>.